

HNF1 α controls glucagon secretion in pancreatic α -cells through modulation of SGLT1

Yoshifumi Sato^{a,1}, Md Mostafizur Rahman^{a,1}, Masaki Haneda^{a,1}, Tomonori Tsuyama^e, Tomoya Mizumoto^a, Tatsuya Yoshizawa^a, Tadahiro Kitamura^b, Frank J. Gonzalez^c, Ken-ichi Yamamura^d, Kazuya Yamagata^{a,e,*}

^a Department of Medical Biochemistry, Faculty of Life Sciences, Kumamoto University, Kumamoto 860-8556, Japan

^b Metabolic Signal Research Center, Institute for Molecular and Cellular Regulation, Gunma University, Maebashi, Gunma, Japan

^c Laboratory of Metabolism, Center for Cancer Research, National Cancer Institute, National Institutes of Health, Bethesda, MD, United States

^d Institute of Resource Development and Analysis, Kumamoto University, 2-2-1 Honjo, Chuo-ku, Kumamoto 860-0811, Japan.

^e Center for Metabolic Regulation of Healthy Aging (CMHA), Faculty of Life Sciences, Kumamoto University, Kumamoto 860-8556, Japan

ARTICLE INFO

Keywords:

Hepatocyte nuclear factor (HNF) 1 α
Maturity-onset diabetes of the young (MODY)
Pancreatic α -cell
Glucagon
Sodium-glucose cotransporter (SGLT)

ABSTRACT

Hepatocyte nuclear factor 1 α (HNF1 α) is a transcription factor required for normal insulin secretion and maintenance of β -cell number in the pancreas. HNF1 α is also expressed in pancreatic α -cells, but its role in these cells is unknown. The aim of this study was to clarify the role of HNF1 α in α -cells. Male *Hnf1a* +/+ mice with a mixed background were backcrossed to outbred ICR mice. Glucose tolerance, glucagon and insulin secretion, islet histology, and gene expression were investigated in ICR *Hnf1a* -/- and *Hnf1a* +/+ mice. Regulation of *Slc5a1* (encoding sodium glucose cotransporter 1 [SGLT1]) expression by HNF1 α and the effect of SGLT1 inhibition on glucagon secretion were also explored. ICR *Hnf1a* -/- mice were glucose intolerant and exhibited impaired glucose-stimulated insulin secretion. The β -cell area of ICR mice was decreased in *Hnf1a* -/- mice, but the α -cell area in the pancreas was similar between *Hnf1a* -/- and *Hnf1a* +/+ mice. *Hnf1a* -/- mice showed higher fasting glucagon levels and exhibited inadequate suppression of glucagon after glucose load. In addition, glucagon release in response to hypoglycemia was impaired in *Hnf1a* -/- mice, and glucagon secretion after 1.1 mM glucose administration, was also decreased in *Hnf1a* -/- islets. *Slc5a1* expression was decreased in *Hnf1a* -/- islets, while HNF1 α activated the *Slc5a1* promoter in α TC1-6 cells. Inhibition of SGLT1 suppressed 1.1 mM glucose-stimulated glucagon secretion in islets and α TC1-6 cells, but SGLT1 inhibition had no additional inhibitory effect in HNF1 α -deficient cells. Our findings indicate that HNF1 α modulates glucagon secretion in α -cells through the regulation of *Slc5a1*.

1. Introduction

Hepatocyte nuclear factor 1 α (HNF1 α), a transcription factor belonging to the homeodomain superfamily, is expressed in the liver, kidney, intestine, and pancreas (including β -cells) [1]. We identified that heterogenous mutations in the gene encoding HNF1 α as a cause of a form of maturity-onset diabetes of the young (MODY3) [2], which is characterized by the progressive impairment of insulin secretion [3,4]. *Hnf1a*-null (-/-) mice and transgenic mice expressing a naturally occurring human dominant-negative P291fsinsC *HNF1A* mutation in pancreatic β -cells develop early-onset diabetes with impaired insulin

secretion and a reduction of β -cell number [5,6]. These results indicate that HNF1 α is required for normal insulin secretion and the maintenance of β -cell number.

Glucagon, which is secreted from pancreatic α -cells, counters the actions of insulin and corrects hypoglycemia by enhancing hepatic glucose output [7,8]. Glucagon secretion is stimulated by hypoglycemia and is suppressed by hyperglycemia and intra-islet paracrine factors, including insulin. We previously demonstrated that HNF1 α is also expressed in glucagon-producing pancreatic α -cells [9], and Haliyur et al. [10], recently reported that glucagon release after stimulation with low glucose and epinephrine was abrogated in human islets expressing an

Abbreviations: HNF, hepatocyte nuclear factor; MODY, maturity-onset diabetes of the young; ICCs, islet-like cell clusters; SGLT, sodium-glucose cotransporter

* Corresponding author at: Department of Medical Biochemistry, Faculty of Life Sciences, Kumamoto University, Kumamoto 860-8556, Japan.

E-mail address: k-yamaga@kumamoto-u.ac.jp (K. Yamagata).

¹ These authors contributed equally to this work.

<https://doi.org/10.1016/j.bbadis.2020.165898>

Received 17 January 2020; Received in revised form 30 June 2020; Accepted 15 July 2020

Available online 22 July 2020

0925-4439/ © 2020 Elsevier B.V. All rights reserved.

HNF1A variant. To clarify the role of HNF1 α in pancreatic α -cells, we investigated the number of pancreatic α -cells and glucagon secretion in *Hnf1a* $^{-/-}$ mice on an outbred ICR background because *Hnf1a* $^{-/-}$ mice on a C57BL/6J background showed early postnatal lethality. In contrast to the decreased β -cell area in *Hnf1a* $^{-/-}$ mice, the total area of glucagon-positive α -cells was similar between control and *Hnf1a* $^{-/-}$ mice. However, *Hnf1a* $^{-/-}$ mice exhibited defective glucagon secretion at low glucose and impaired suppression of glucagon secretion at high glucose. Sodium glucose cotransporter 1 (SGLT1), a glucose transporter expressed in pancreatic α -cells, controls glucagon secretion [11]. We found that HNF1 α regulated the transcription of *Slc5a1* (encoding SGLT1) in α -cells, and that SGLT1 expression was decreased in *Hnf1a* $^{-/-}$ islets. Furthermore, inhibition of SGLT1 suppressed glucagon secretion at low glucose, but SGLT1 inhibition had no additional inhibitory effect in HNF1 α -deficient cells. Our findings indicate that HNF1 α plays an important role in glucagon secretion in α -cells, and the decreased expression of SGLT1 might be involved, at least in part, in the dysregulated secretion of glucagon.

2. Materials and methods

2.1. Cell culture

Mouse α TC1 clone 6 (α TC1-6, CRL-2934) cells were obtained from the American Type Culture Collection (Manassas, VA). The cells were maintained at 37 °C in a 5% (v/v) CO₂ incubator in Dulbecco's modified Eagle's medium containing 25 mM glucose, 44 mM sodium bicarbonate, 10% (v/v) fetal bovine serum, 15 mM HEPES, 0.1 mM nonessential amino acids, and antibiotics (50 U/mL penicillin and 50 U/mL streptomycin). Islets isolated from mice were cultured in RPMI-1640 medium (Gibco, Grand Island, NY) including 10% (v/v) fetal bovine serum, HEPES, sodium pyruvate, and antibiotics.

2.2. Mouse models

Hnf1a $^{+/-}$ mice (MGI:2384429) [12] with a mixed background (129Svj \times C57BL/6J \times FVB/N) were backcrossed to C57BL/6J or ICR mice (KBT Oriental Co., Ltd., Saga, Japan) for at least six generations before their use in this study. Another line of *Hnf1a* $^{+/-}$ mice on a C57BL/6J background was produced as previously described [13,14]. A targeting vector was constructed containing 6.25 kb of the 5' homologous region and 3.24 kb of the 3' homologous region flanking the initiation ATG codon in exon 1 of *Hnf1a*. We used a RENKA embryonic stem (ES) cell line derived from C57BL/6 mice [15]. Heterozygous *Hnf1a* $^{+/-}$ mice were crossed to generate *Hnf1a* $^{-/-}$ mice. The percentage of *Hnf1a* $^{+/+}$, *Hnf1a* $^{+/-}$, and *Hnf1a* $^{-/-}$ mice that survived for more than 10 days after birth was calculated. The survival rates between genotypes were analyzed by the Kaplan-Meier method. The mice were maintained under specific pathogen-free conditions in a 12-h light (07:00–19:00)/12-h dark (19:00–07:00) cycle with free access to water and normal mouse chow (CE-2; CLEA, Tokyo, Japan). To maintain the survival of newborn *Hnf1a* $^{-/-}$ pups, pregnant female mice were fed a pelleted commercial diet (CMF; Oriental Yeast Co., Ltd., Tokyo, Japan) until they gave birth and their pups were weaned. Room temperature was maintained at 22 \pm 1–2 °C. The handling and killing of the mice were performed in compliance with the animal care guidelines of Kumamoto University. This research was approved by the animal research committee of Kumamoto University, and all animal experimental procedures were approved by the Kumamoto University Ethics Review Committee for Animal Experimentation.

2.3. Metabolic parameters and metabolic studies

Body weights and plasma glucose levels were measured in mice aged from 3 to 20 weeks. After a 6-h (for an intraperitoneal glucose tolerance test [IPGTT]) and glucose-stimulated insulin secretion [GSIS]

test) and 4-h (for an insulin tolerance test [ITT]) fasting period, 3- to 8-week-old mice were intraperitoneally administered either 2 g/kg glucose (for IPGTT), 3 g/kg glucose (for GSIS), or 2.0 U/kg human insulin (Humulin-R; Eli Lilly and Co., Indianapolis, IN) (for ITT). Blood glucose was measured by a glucose sensor (Glutest Neo Super; Sanwa Kagaku, Nagoya, Japan). Tail blood was collected at the indicated times, and aprotinin (250 KIU/mL) and EDTA (0.75 mg/mL) were added to blood samples for plasma glucagon measurements. Plasma insulin and glucagon levels were determined using a mouse insulin enzyme-linked immunosorbent assay (ELISA) kit (type S) (Shibayagi Co., Gunma, Japan) and a mouse glucagon ELISA kit (Mercodia AB, Uppsala, Sweden).

2.4. Histology

Pancreas tissues from *ad libitum*-fed mice were fixed with 10% (v/v) neutral buffered formalin (Wako Pure Chemical Industries, Ltd.) for 18–24 h at 4 °C. Fixed samples were embedded in paraffin, cut into 10- μ m cross-sections, mounted on MAS-coated slides (Matsunami Glass, Osaka, Japan), and deparaffinized for standard histological staining with hematoxylin and eosin (HE). Six paraffin-embedded pancreas sections cut at 100- μ m intervals were stained with HE, and the pancreatic islet area of each section was circled and calculated by using ImageJ software (US National Institutes of Health, Bethesda, MD). The distribution of islet size was categorized based on islet area (μ m²).

2.5. Immunofluorescence and cell distribution analysis

To determine the α - or β -cell composition of each islet, 10 μ m-thick paraffin-embedded pancreas sections were subjected to antigen retrieval using HistoVT One (L6F9587; Nacalai Tesque, Kyoto, Japan), and double-stained with an anti-insulin antibody (A0564, 1:400; Dako, Santa Clara, CA) and anti-glucagon antibody (#ab92517, 1:400; Abcam, Cambridge, MA). After reaction with fluorescent dye-conjugated secondary antibodies, fluorescent signals were captured using an all-in-one fluorescent microscope (BZ-X700; Keyence, Tokyo, Japan). The total area (μ m²), glucagon-positive area (μ m²), and insulin-positive area (μ m²) of each islet was measured by Keyence software. Small islet-like cell clusters (ICCs) were defined as a cell population that is made up of only insulin-positive cells or glucagon-positive cells.

2.6. Islet isolation, glucagon content, and glucagon secretion

Pancreatic islets were isolated from *Hnf1a* $^{+/+}$ and *Hnf1a* $^{-/-}$ mice as previously described [16]. Briefly, after bile duct cannulation and digestion of the pancreas using a mixture of 1.5 mg/mL collagenase L (Nitta Gelatin, Osaka, Japan), 1.5 mg/mL hyaluronidase (H3506; Sigma-Aldrich, St. Louis, MO), and 0.1% (v/v) protease inhibitor cocktail (Nacalai Tesque, Inc., Kyoto, Japan), isolated islets were manually collected. Islet glucagon was extracted by an acid-ethanol extraction method as previously described [17]. To assess glucagon secretion from isolated islets *in vitro*, size-matched islets were pre-incubated in pH 7.4 HEPES-buffered Krebs-Ringer bicarbonate solution (KRBH) buffer (120 mM NaCl, 4.7 mM KCl, 1.2 mM KH₂PO₄, 2.4 mM CaCl₂, 1.2 mM MgCl₂, 20 mM NaHCO₃, and 10 mM HEPES) containing 11 mM glucose and then stimulated with KRBH buffer containing 1.1 or 5.6 mM glucose, or with 20 mM KCl for the indicated time. To examine the effect of SGLT inhibition on glucagon secretion, isolated islets were pre-incubated with 20 μ M sotagliflozin for 2 h, after which a glucagon secretion assay was performed in the presence of 20 μ M sotagliflozin. Glucagon concentration was determined by a mouse glucagon enzyme-linked immunosorbent assay (ELISA) kit (Mercodia AB, Uppsala, Sweden) and glucagon levels were normalized by islet number.

2.7. Western blotting

Western blotting analysis was performed as previously described [18]. Twenty µg of total protein lysates from isolated islets and αTC1-6 cells were subjected to gel electrophoresis and protein transfer onto PVDF membrane. The following primary antibodies were used: anti-HNF1α (610,902; BD Biosciences, San Jose, CA), anti-β-actin (clone AC15; Sigma-Aldrich), and anti-SGLT1 (#ab14685; Abcam). After reaction with secondary antibodies, the signals were detected by using Chemi-Lumi One Super type (Nacalai Tesque) and a ChemiDoc imaging system (BR170-8265; Bio-Rad Laboratories, Hercules, CA).

2.8. Quantitative real-time RT-PCR

Liver tissues and αTC1-6 cells were homogenized in Sepasol-RNA I Super G solution (Nacalai Tesque), and total RNA was isolated using a conventional phenol-chloroform-based RNA extraction method. Pancreatic islet RNA was purified with an RNeasy Micro Kit (Qiagen, Valencia, CA). cDNA was prepared using a PrimeScript RT reagent kit and gDNA Eraser (RR047A; TaKaRa Bio, Inc., Shiga, Japan). Quantitative PCR (qPCR) was performed using SYBR Premix Ex Taq II (RR820A; TaKaRa Bio, Inc.) and an ABI 7300 thermal cycler (Applied Biosystems, Foster City, CA). For each gene, mRNA levels were determined by the comparative Cycle threshold (Ct) method ($\Delta\Delta C_t$) and levels of each mRNA were normalized to 18S rRNA or TATA-binding protein (*Tbp*) mRNA. Primer sequences for *Cltn*, *Slc2a2*, *Hnf4a*, *Hgf*, *Agxt*, *G6pc*, *Got1*, *Sglt1*, *Sglt2*, and *Slc5a1* mRNAs are listed in Supplementary Table 1.

2.9. Chromatin immunoprecipitation quantitative real-time PCR (ChIP qPCR)

αTC1-6 cells were fixed in 1% formaldehyde at room temperature and the reaction was quenched by 150 mM glycine. The fixed cells were incubated in 0.5% Nonidet P-40 buffer on ice for 15 min and lysed in SDS lysis buffer (50 mM Tris-HCl, pH 8.0, 1% SDS, and 10 mM EDTA). DNA was sheared using a Bioruptor Sonicator (Diagenode, Denville, NJ) by 7 cycles of sonication (30 s on, 30 s off, high output). The sheared chromatin was diluted 5-fold in ChIP dilution buffer (50 mM Tris-HCl, pH 8.0, 167 mM NaCl, 1.1% Triton X-100, and 0.11% sodium deoxycholate). The chromatin was incubated with 2 µg anti-HNF1 antibody (sc-8986; Santa Cruz Biotechnology, Dallas, TX) or control IgG (2729; Cell Signaling Technology, Danvers, MA) overnight at 4 °C. The chromatin was incubated with magnetic beads (Dynabeads protein A and protein G; Invitrogen, Carlsbad, CA) for 6 h at 4 °C, followed by sequential washing with low-salt RIPA buffer (50 mM Tris-HCl, pH 8.0, 150 mM NaCl, 1 mM EDTA, 0.1% SDS, 1% Triton X-100, and 0.1% sodium deoxycholate), high-salt RIPA buffer (50 mM Tris-HCl, pH 8.0, 500 mM NaCl, 1 mM EDTA, 0.1% SDS, 1% Triton X-100, and 0.1% sodium deoxycholate), LiCl wash buffer (10 mM Tris-HCl, pH 8.0, 250 mM LiCl, 1 mM EDTA, 0.5% Nonidet P-40, and 0.5% sodium deoxycholate), and Tris-EDTA buffer. The chromatin was eluted and reverse cross-linked in ChIP direct elution buffer (50 mM Tris-HCl, pH 8.0, 5 mM EDTA, and 0.5% SDS) overnight at 65 °C. DNA fragments, which were manually extracted and collected by using phenol-chloroform extraction and ethanol precipitation, were evaluated by qPCR with primers for the *Tbp* gene body (P1) (5'-CCCCTGTACCCTTACC AAT-3' and 5'-GAAGCTGCGGTACAATTCCAG-3'), primers for the *Slc5a1* promoter region without the HNF1 binding motif (P2) (5'-TTG TCTCTTGCTCTTTGAGG-3' and 5'-GGTGATGTTTCATAGCTTGC-3'), and primers for the *Slc5a1* promoter region containing the HNF1 binding motif (P3) (5'-ACACCTAGGAGCTGCTTCC-3' and 5'-TCAAGG TGCTACTGTCCATG-3').

2.10. Retrovirus-mediated transduction of short hairpin RNA (shRNA) and small interfering RNA (siRNA) transfection

For knocking down *Hnf1a* expression, a specific shRNA target sequence (5'-GCCTAATGGCCTTGGAGAAAC-3') was designed for mouse *Hnf1a* using the BLOCK-iT™ RNAi Designer (Thermo Fisher Scientific, Waltham, MA). Oligonucleotides encoding shRNA were cloned into a pSIREN-RetroQ shRNA expression vector (Clontech Laboratories, Inc., Mountain View, CA). Then, the pSIREN-RetroQ control vector or pSIREN-RetroQ-*Hnf1a* vector was transfected into Plat-E cells, a retroviral packaging cell line, using the jetPRIME reagent (Polyplus, New York, NY). αTC1-6 cells were infected with retrovirus-containing medium and selected by incubation with 5 µg/mL puromycin to generate αTC1-6 cells stably expressing HNF1α shRNA (HNF1α KD αTC1-6 cells) or negative control shRNA (control αTC1-6 cells). For *Slc5a1* knockdown, αTC1-6 cells (3.0×10^5 cells, 24-well plate) were transfected with control scramble siRNA or mouse *Slc5a1* Silencer Select siRNA (s73953, Ambion; Thermo Fisher Scientific) at a final concentration of 10 nM using the Lipofectamine RNAiMAX reagent (Thermo Fisher Scientific), according to the manufacturer's instructions.

2.11. Transient transfection and luciferase reporter assay

The mouse *Sglt1* promoter containing a putative HNF1α binding site was amplified by PCR using a pair of primers (5'-AACTCGAGGCAGAC TCTCTTGAG-3' and 5'-AAGCTGGGATGGGTGCATCGGTGGCAGT AAC-3'), and it was sub-cloned into the pGL4.10 basic reporter (Promega, Madison, WI). The transcription factor binding site was altered by PCR-based mutagenesis using a pair of primers (5'-GCTGTTA ACTCAAAGCAGTATAAG-3' and 5'-CAGCCCCGAGGGAG-3') to produce an HNF1α binding site mutant (CTGGCTGTTAAC). The pcDNA3.1-wild-type (WT)-HNF1α and pcDNA3.1-P291fsinsC mutant-HNF1α expression plasmids were previously described [19]. αTC1-6 cells (2.0×10^5 cells) were seeded into each well of a 48-well plate at 24 h before transfection. Transient transfection was performed using the jetPRIME reagent (Polyplus) according to the manufacturer's instructions. At 24 or 48 h after transfection, luciferase activity was measured by using a Dual-Luciferase reporter assay system (Promega).

2.12. Glucose uptake assay

Size-matched islets isolated from *Hnf1a*^{+/+} and *Hnf1a*^{-/-} mice were pre-cultured in RPMI-1640 medium with DMSO or 20 µM sotagliflozin (LX4211; Cayman Chemical, Ann Arbor, MI) for 2 h. After washing once with KRBH buffer containing 1.1 mM glucose, they were incubated in KRBH buffer containing 1.1 mM glucose, 200 µM of 2-[N-(7-nitrobenz-2-oxa-1,3-diazol-4-yl)amino]-2-deoxyglucose (2-NBDG, Peptide Institute, Osaka, Japan), and DMSO or 20 µM sotagliflozin for 1 h. After washing with KRBH buffer, images were captured by an all-in-one fluorescence microscope (BZ-X700; Keyence, Osaka, Japan) and fluorescence intensity in the peripheral area (approximately 50% outside of the radius) of the islets was measured.

2.13. Statistical analysis

Data are presented as mean values ± standard error (S.E.) of the mean of the indicated number of experiments (n). The significance of differences was assessed with an unpaired *t*-test and a log-rank (Mantel-Cox) test, and a value of *p* < 0.05 was considered to be statistically significant.

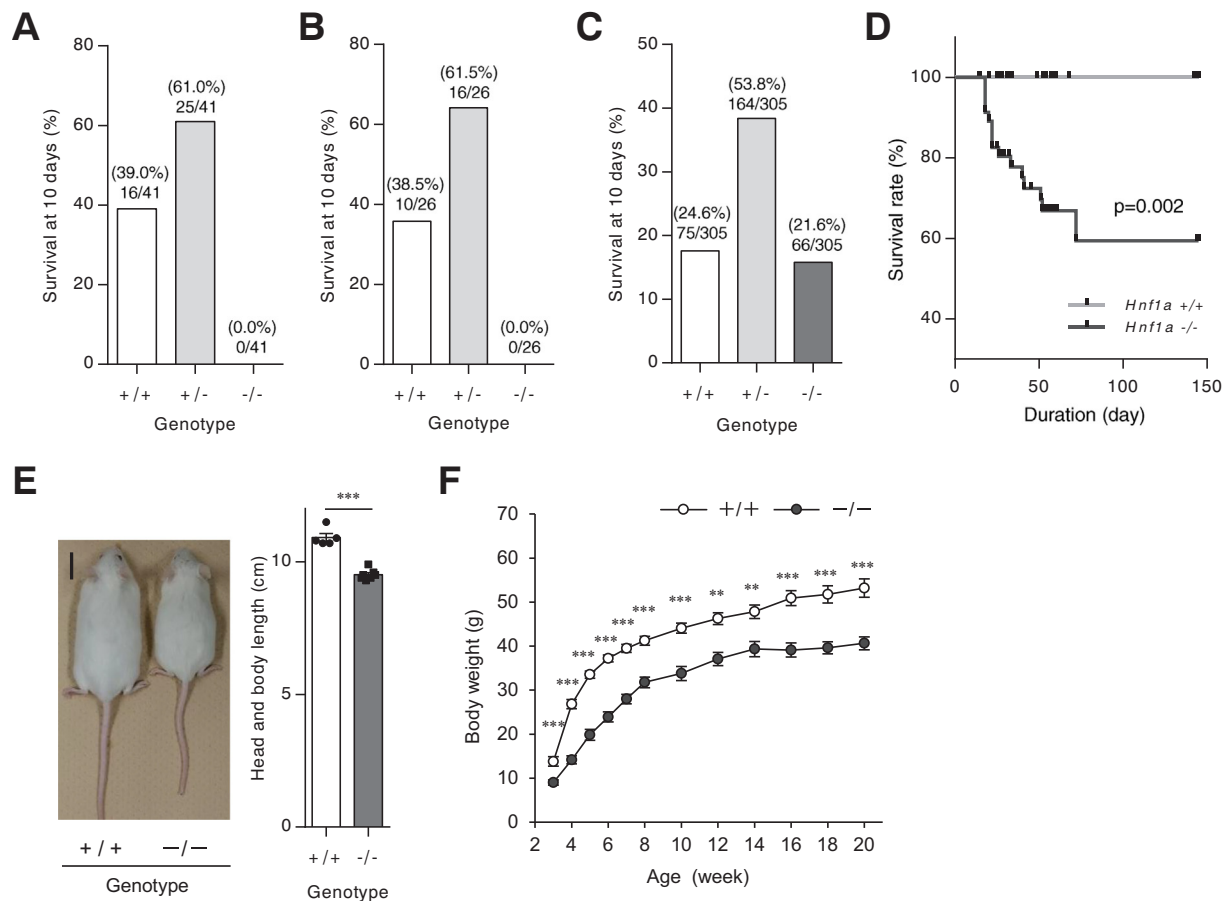


Fig. 1. Phenotypic analyses of *Hnf1a*^{-/-} mice on the ICR background. (A–C) Genotypic distribution at 10 days after birth. The number of *Hnf1a* wild-type (+/+), *Hnf1a* heterozygous (+/-), and *Hnf1a* null (-/-) mice born after being backcrossed 6 times with C57BL/6J mice (A), or with a pure C57BL/6J background (B), or born after being backcrossed 6 times with ICR mice (C) was counted (3–5 generations). The ratio on the bars indicates genotype-matched mouse number/total mouse number from multiple litters. (D) Kaplan-Meier survival curves for *Hnf1a* +/+ (n = 39; gray) and *Hnf1a* -/- (n = 66; black) littermates. p values were calculated using a log-rank (Mantel-Cox) test. (E) Gross appearance of 10-week-old *Hnf1a* +/+ (left) and *Hnf1a* -/- (right) mice. Scale bar, 2 cm. Body length (from the tip of the nose to the base of the tail) (n = 5–7) was measured. (F) Body weight chart for male *Hnf1a* +/+ (n = 63) and *Hnf1a* -/- (n = 65) mice from 3 to 20 weeks of age. All data are presented as mean ± S.E. (S.E.; error bars). **p < 0.01, ***p < 0.001.

3. Results

3.1. Generation of *Hnf1a*^{-/-} mice with an ICR background

To clarify the role of HNF1 α in pancreatic α -cells, heterozygous *Hnf1a* +/+ mice (mixed background of 129Svj \times C57BL/6J \times FVB/N) [12] were crossed over six generations to generate a pure C57BL/6J background. C57BL/6J *Hnf1a* -/- mice were not embryonic lethal, but none of the *Hnf1a* -/- newborns lived for longer than 10 days (Fig. 1A). The early postnatal lethality of *Hnf1a* -/- mice with the C57BL/6J background was also detected in another line of *Hnf1a* -/- mice [13] (Fig. 1B). Since postnatal lethality in an inbred strain can often be rescued in an outbred line [20,21], *Hnf1a* +/+ mice with a mixed background [12] were backcrossed to outbred ICR mice for 6 generations. On the ICR background, most of the *Hnf1a* -/- mice lived more than 10 days (observed ratio at 10 days: *Hnf1a* +/+ 24.6%, *Hnf1a* +/- 53.8%, *Hnf1a* -/- 21.6%) (Fig. 1C). The survival rate of *Hnf1a* null mice on the ICR background (ICR *Hnf1a* -/- mice) gradually decreased, but these mice still lived longer than previously reported *Hnf1a* -/- mice (Fig. 1D) [22]. ICR *Hnf1a* -/- mice were smaller than *Hnf1a* +/+ mice, and body weight was significantly lower in *Hnf1a* -/- mice relative to control mice (Fig. 1E, F), as previously described [12,22]. The liver of ICR *Hnf1a* -/- mice showed increased triglyceride and glycogen content compared with *Hnf1a* +/+ mice (Supplementary Fig. 1), consistent with previous reports [12,22–24].

3.2. Defective insulin secretion in ICR *Hnf1a*^{-/-} mice

Diabetic phenotype, pancreatic islet size, and β -cell mass are reported to be profoundly affected by genetic background in *Hnf1a* -/- mice [25]. The non-fasting blood glucose levels of ICR *Hnf1a* -/- mice were significantly higher than those of ICR *Hnf1a* +/+ mice after 5 weeks of age (Fig. 2A). Although blood glucose levels were similar between ICR *Hnf1a* +/+ and *Hnf1a* -/- mice at 4 weeks of age, an intraperitoneal glucose tolerance test (IPGTT) demonstrated that ICR *Hnf1a* -/- mice were glucose intolerant at this age (Fig. 2B). As previously reported [5], the insulin secretory response to glucose was significantly impaired in *Hnf1a* -/- mice (Fig. 2C). The expression of *Clnr*, *Hnf4a*, *Slc2a2*, and *Hgf* mRNAs, which are direct target genes of HNF1 α [1,26], was significantly decreased in the islets of *Hnf1a* -/- mice (Fig. 2D). The islets of ICR *Hnf1a* -/- mice were smaller than those of *Hnf1a* +/+ mice (Fig. 2E). These results are consistent with the phenotypes of previously reported *Hnf1a* -/- mice [5].

3.3. Pancreatic β -cells and α -cells in ICR *Hnf1a*^{-/-} mice

Immunohistochemical analysis revealed that the proportion of insulin-positive cells in ICR *Hnf1a* -/- islets was markedly decreased compared with that of ICR *Hnf1a* +/+ islets (Fig. 3A). As previously reported [5], the β -cell area in the islets of ICR *Hnf1a* -/- mice was significantly decreased compared with *Hnf1a* +/+ mice (Fig. 3A, B).

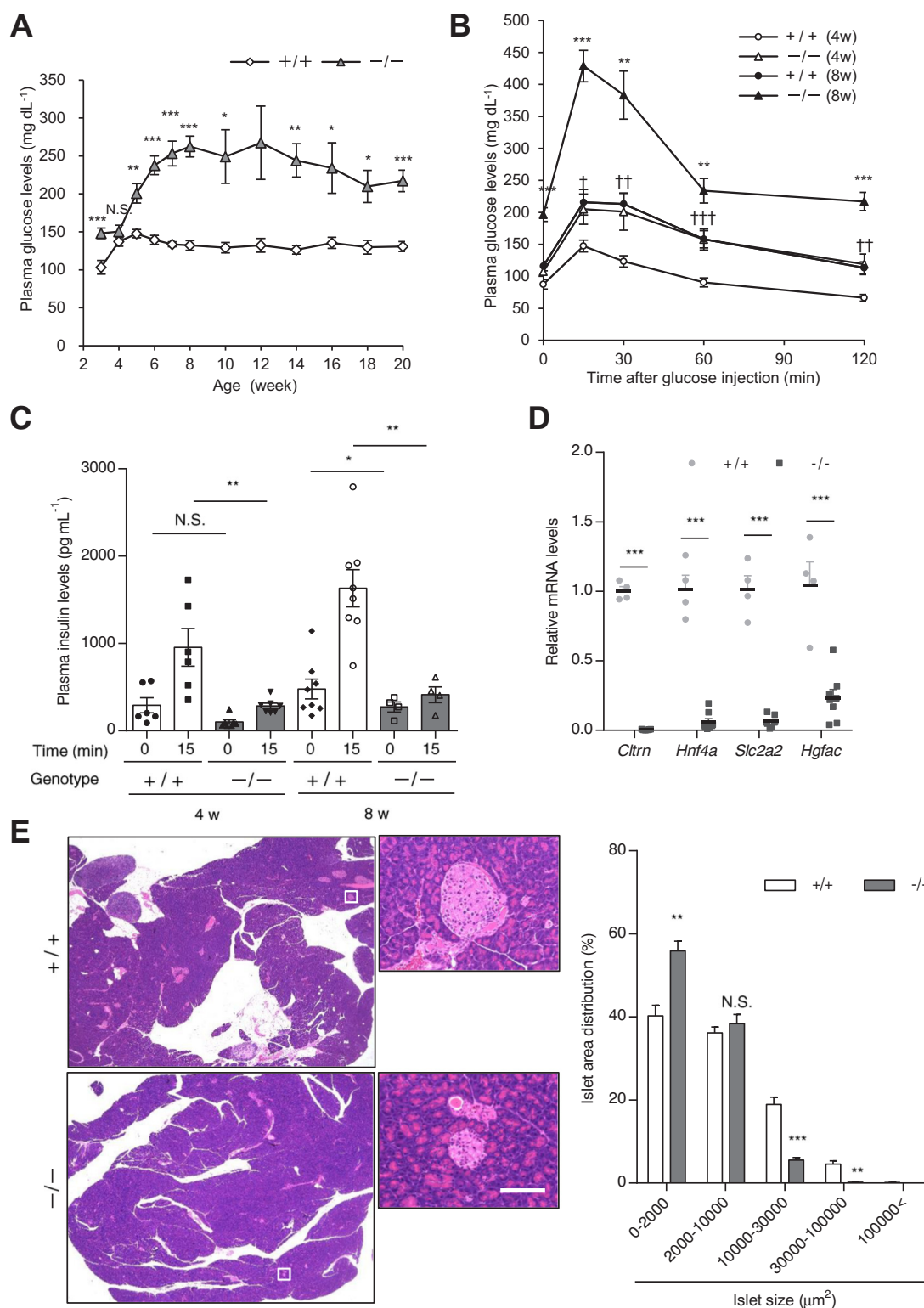


Fig. 2. β -Cell dysfunction in *Hnf1a*^{-/-} mice. (A) Plasma glucose chart for male *Hnf1a*^{+/+} (n = 63) and *Hnf1a*^{-/-} (n = 65) mice from 3 to 20 weeks. (B, C) IPGTT (B) and GSIS (C) of 4- and 8-week-old *Hnf1a*^{+/+} (n = 6–8) and *Hnf1a*^{-/-} (n = 4–7) mice. (D) Islet gene expression of 8-week-old mice was quantified by qPCR (n = 4). The expression levels of *Cltn*, *Hnf4a*, *Slc2a2*, and *Hgf* were normalized to that of *Tbp*. (E) H&E staining of pancreas sections from 8-week-old mice (left). Scale bar, 100 μ m. Profiling of islet size distribution in *Hnf1a*^{+/+} and *Hnf1a*^{-/-} mice (right) (n = 4). +/+ and -/- indicate *Hnf1a*^{+/+} and *Hnf1a*^{-/-} mice, respectively. All data are presented as mean \pm S.E. (S.E.; error bars). N.S., not significant; *p < 0.05; **p < 0.01; ***p < 0.001.

There was also a tendency for a decreased α -cell area in the islets of ICR *Hnf1a*^{-/-} mice, but the difference did not reach statistical significance (Fig. 3B). Due to the decrease of β -cell number, the ratio of α -cells in *Hnf1a*^{-/-} islets was significantly increased compared with

that in *Hnf1a*^{+/+} islets (Fig. 3C). A comparison of similarly sized islets (total islet area, 500–2000 μ m²) also revealed that the ratio of α -cells was significantly increased in *Hnf1a*^{-/-} islets compared with *Hnf1a*^{+/+} islets (Supplementary Fig. 2). Small islet-like cell clusters (ICCs),

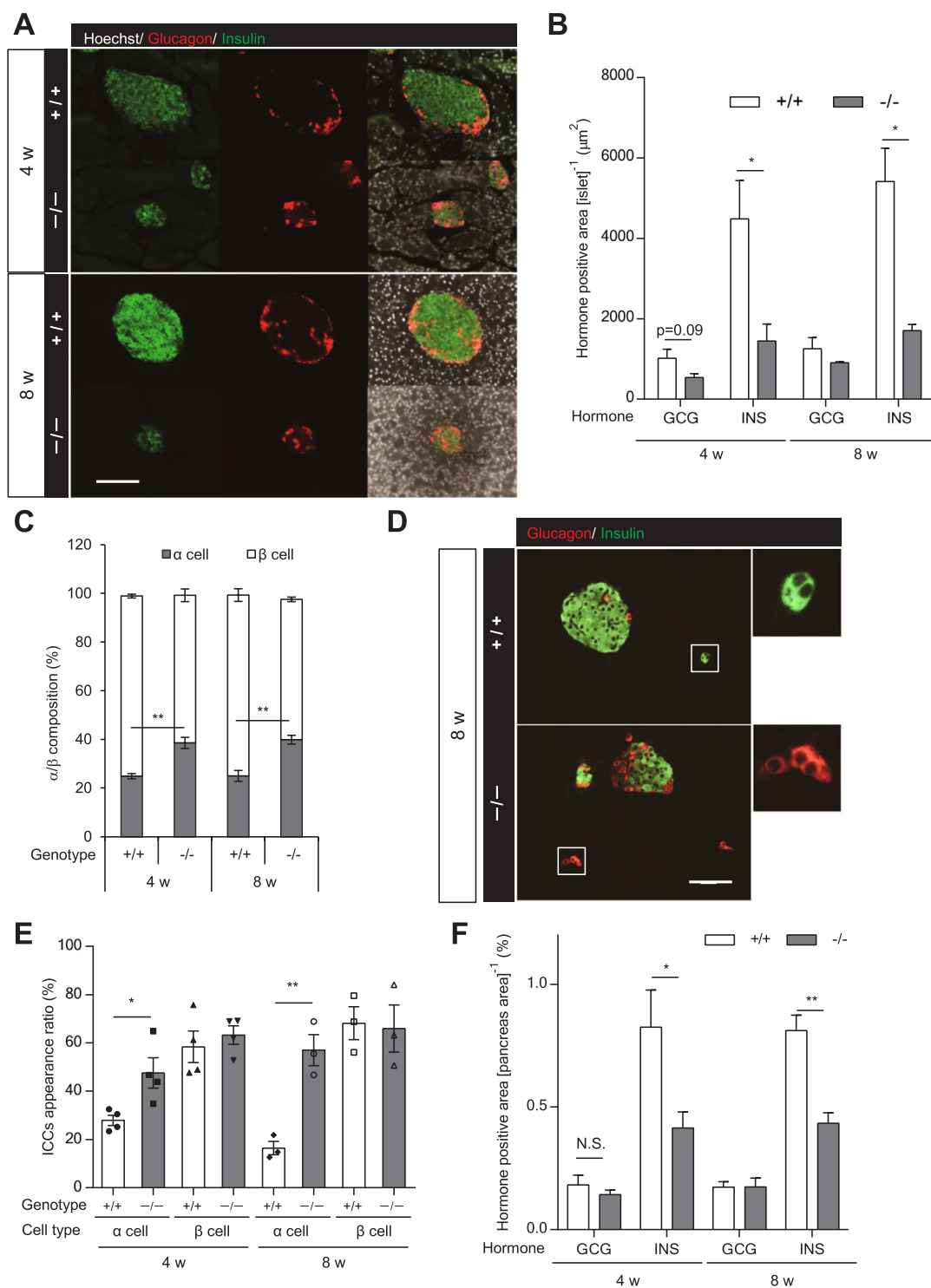


Fig. 3. Islet cell composition and α -cell area in the pancreas of *Hnf1a*^{-/-} mice. (A) α -cell and β -cell composition in each islet of 4- and 8-week-old mice. Immunofluorescence for insulin (green), glucagon (red), and Hoechst (white). Scale bars, 100 μ m. (B) Glucagon (GCG)-positive and insulin (INS)-positive areas (μ m²) in the islet area on the section were measured (n = 3–4). (C) Percentage of α -cell area and β -cell area to islet total area is shown (n = 3–4). (D) Representative image of ICCs in 8-week-old mouse pancreas. Immunofluorescence for insulin (green) and glucagon (red). Scale bars, 100 μ m. (E) Appearance ratio of ICCs in 4- and 8-week-old mouse pancreas (n = 3–4). (F) Glucagon (GCG)-positive and insulin (INS)-positive areas in the whole pancreas area on the section were calculated (n = 3–6). +/+ and -/- indicate *Hnf1a*^{+/+} and *Hnf1a*^{-/-} mice, respectively. All data are presented as mean \pm S.E. (S.E.; error bars). N.S., not significant; *p < 0.05; **p < 0.01.

which consist exclusively of insulin-positive cells or glucagon-positive cells, were occasionally detected in the pancreas (Fig. 3D). The appearance rate of ICCs, consisting of only insulin-positive cells, was similar between *Hnf1a*^{-/-} and *Hnf1a*^{+/+} mice, but the appearance rate of ICCs consisting exclusively of glucagon-positive cells was

significantly increased in *Hnf1a*^{-/-} mice (Fig. 3E). Collectively, the α -cell area in the pancreas was similar between *Hnf1a*^{-/-} and *Hnf1a*^{+/+} mice, even though the islets were smaller in *Hnf1a*^{-/-} mice (Fig. 3F).

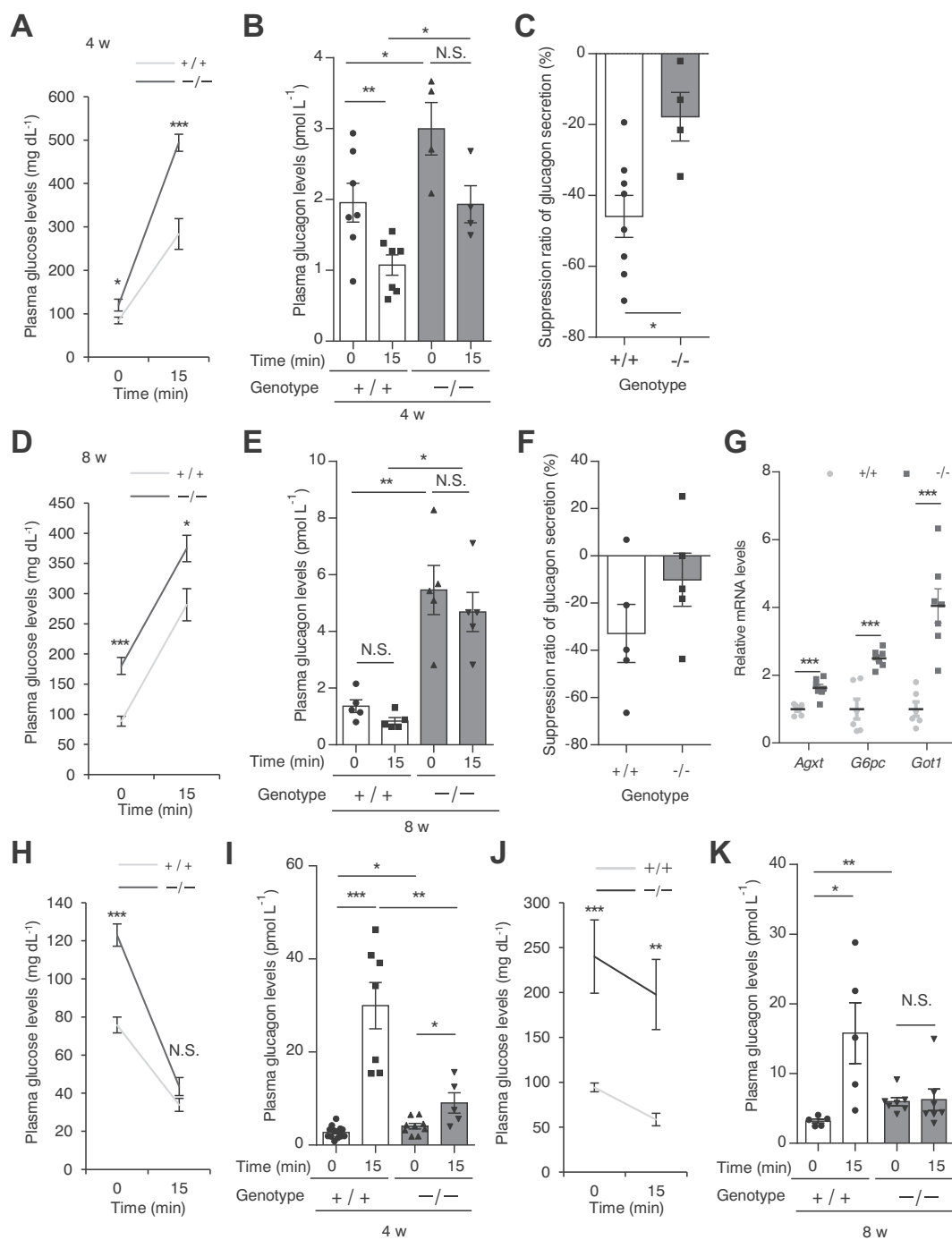


Fig. 4. Dysregulated glucagon secretion in *Hnf1a*^{-/-} mice (A–F). Plasma glucose levels (A, D) and plasma glucagon levels (B, E) before and at 15 min after glucose injection (3 g/kg) of 4- and 8-week-old *Hnf1a*^{+/+} (n = 5–7) and *Hnf1a*^{-/-} (n = 4–5) mice. Suppression ratio of glucagon secretion (15 min after glucose injection vs. 0 min) in 4- and 8-week-old *Hnf1a*^{+/+} (n = 5–8) and *Hnf1a*^{-/-} (n = 4–5) mice (C, F). (G) Hepatic gene expression of glucagon target genes in 8-week-old *ad libitum*-fed mice. The expression levels of *Agxt*, *G6pc*, and *Got1* were normalized to that of *18S rRNA* (n = 6–7). (H–K) Plasma glucose levels (H, J) and plasma glucagon levels (I, K) before and at 15 min after human insulin injection (2.0 U/kg) of 4-week-old mice (H, I) and 8-week-old mice (J, K) of both genotypes (n = 5–15). *+/+* and *-/-* indicate *Hnf1a*^{+/+} and *Hnf1a*^{-/-} mice, respectively. All data are presented as mean ± S.E. (S.E.; error bars). N.S., not significant; *p < 0.05; **p < 0.01; ***p < 0.001.

3.4. Dysregulation of glucagon secretion in ICR *Hnf1a*^{-/-} mice

To address the functional impact of the loss of HNF1α in pancreatic α-cells, we examined glucagon secretion in response to the intraperitoneal administration of glucose in 4- and 8-week-old ICR *Hnf1a*^{-/-} mice. ICR *Hnf1a*^{-/-} mice showed higher fasting blood glucose levels (Fig. 4A, D) and plasma glucagon levels (Fig. 4B, E) compared with *Hnf1a*^{+/+} mice at both ages. Plasma glucagon levels

were significantly decreased after intraperitoneal glucose load in 4-week-old *Hnf1a*^{+/+} mice (Fig. 4B). The suppression of glucagon secretion after glucose load was inhibited in *Hnf1a*^{-/-} mice (*Hnf1a*^{+/+} 46.0%, *Hnf1a*^{-/-} 17.8%, p < 0.05) (Fig. 4C). Hyperglucagonemia in *Hnf1a*^{-/-} mice persisted at 8 weeks of age (Fig. 4E), and there was no significant reduction of plasma glucagon levels between before and after glucose load (Fig. 4E, F). The liver is a major target organ for glucagon action, and glucagon regulates the hepatic

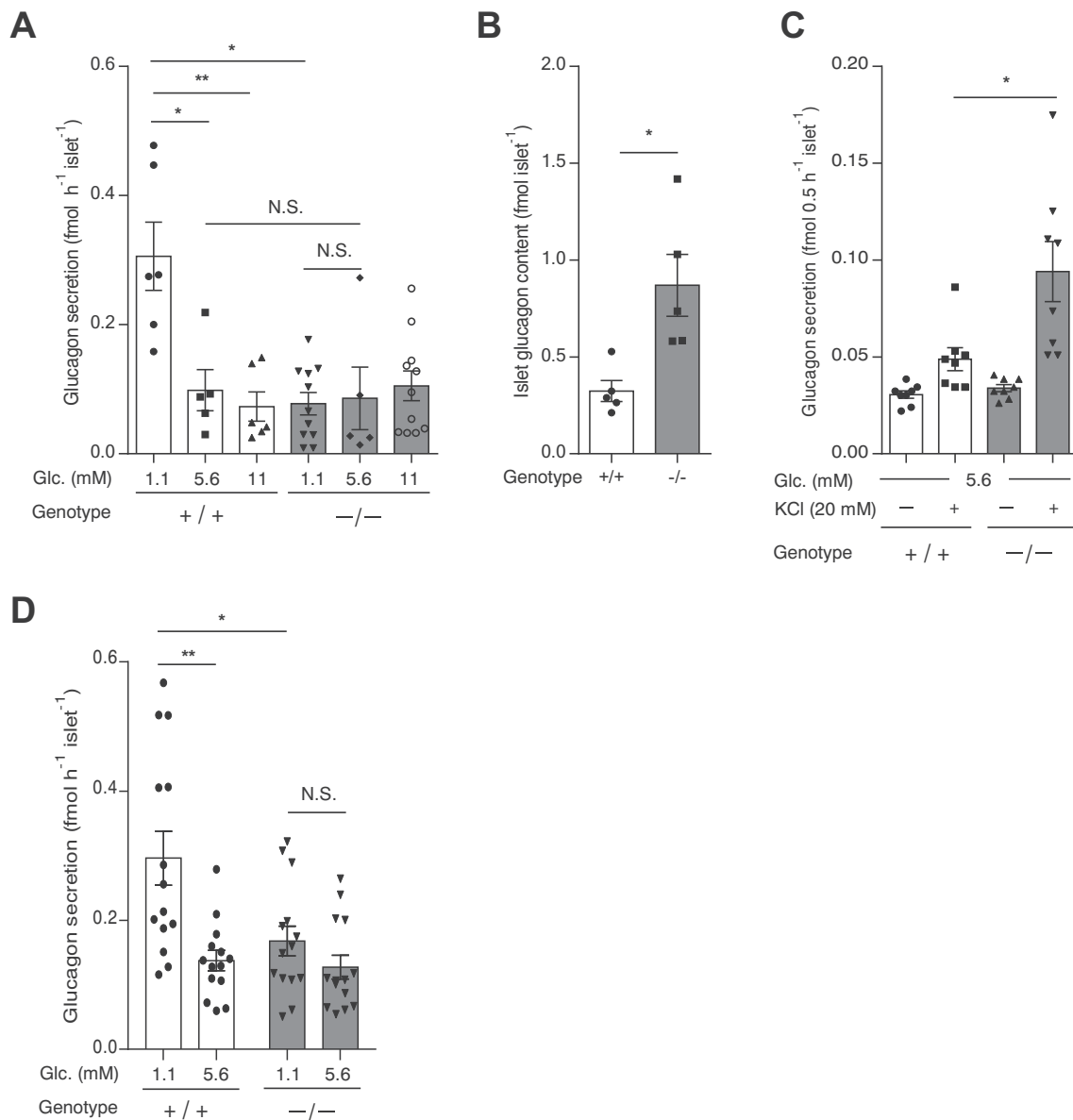


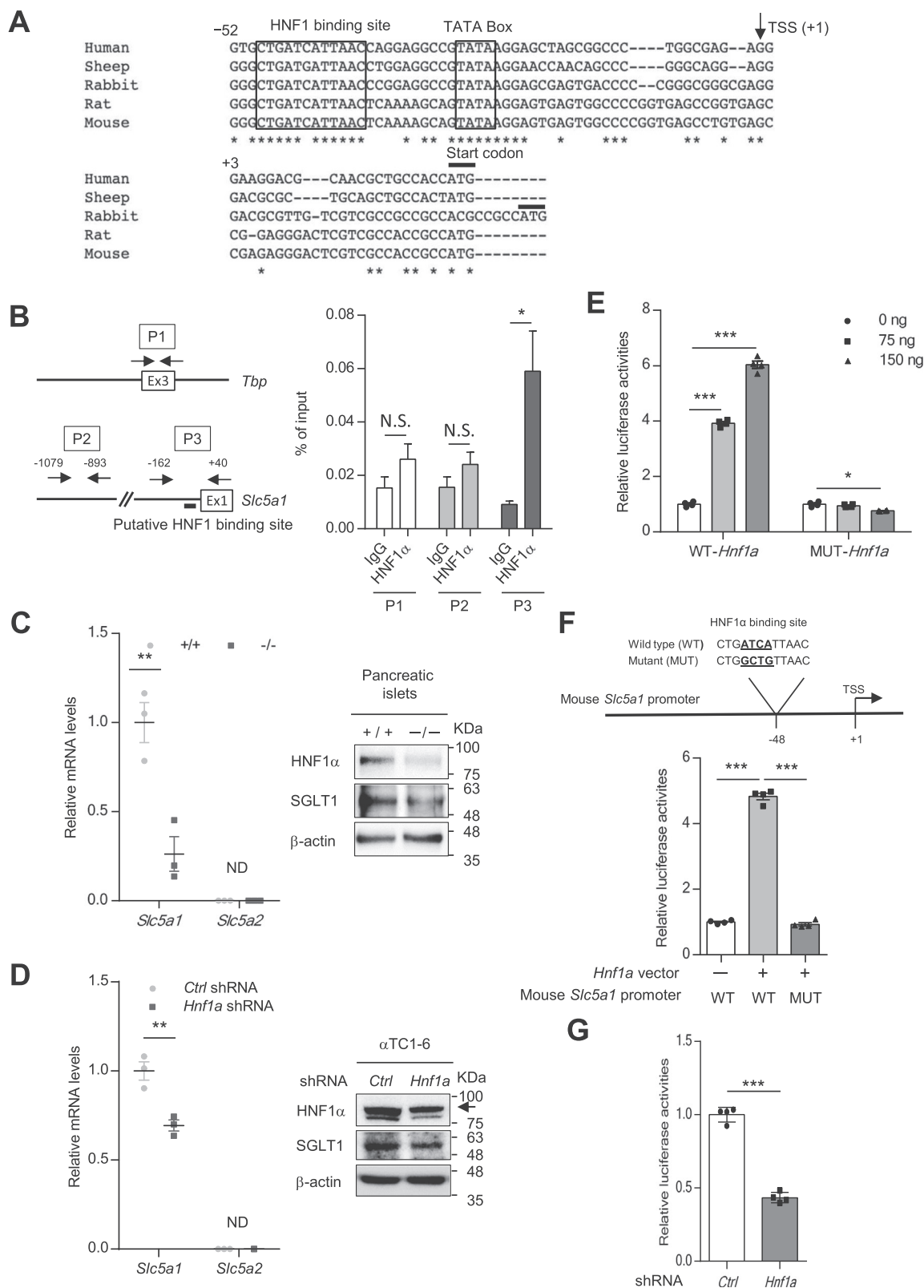
Fig. 5. Glucagon secretion defects in the islets of *Hnf1a*^{-/-} mice. (A) Glucagon secretion in isolated islets from 4-week-old *Hnf1a*^{+/+} and *Hnf1a*^{-/-} mice at 1.1, 5.6, and 11 mM glucose (n = 5–11 experiments using islets from 4 to 5 mice per genotype). (B) Islet glucagon content was normalized to islet number. (C) Glucagon secretion in the isolated islets from 4-week-old *Hnf1a*^{+/+} and *Hnf1a*^{-/-} mice at 5.6 mM glucose with or without 20 mM KCl (n = 8 experiments using islets from 4 to 5 mice per genotype). (D) Glucagon secretion in isolated islets from 8-week-old *Hnf1a*^{+/+} and *Hnf1a*^{-/-} mice at 1.1, and 5.6 mM glucose (n = 14 experiments using islets from 3 to 4 mice per genotype). +/+ and -/- indicate *Hnf1a*^{+/+} and *Hnf1a*^{-/-} mice, respectively. All data are presented as mean ± S.E. (S.E.; error bars). N.S., not significant; *p < 0.05; **p < 0.01.

expression of *Agxt*, *G6pc*, and *Got1* [27]. Consistently, the expression of these genes was significantly increased in the liver of hyperglucagonemic *Hnf1a*^{-/-} mice (Fig. 4G).

We next examined glucagon secretion in response to intraperitoneal insulin injection. Plasma glucagon levels were significantly increased (11.1-fold) by injection of 4-week-old *Hnf1a*^{+/+} mice with insulin (Fig. 4H, I). Notably, this increase of glucagon secretion was significantly impaired in *Hnf1a*^{-/-} mice. Similarly, 8-week-old *Hnf1a*^{-/-} mice also exhibited a lack of glucagon secretion after insulin injection (Fig. 4J, K).

We then investigated glucagon secretion in islets isolated from 4-week-old *Hnf1a*^{+/+} and *Hnf1a*^{-/-} mice. In *Hnf1a*^{+/+} islets, glucagon secretion after 1.1 mM glucose treatment was significantly elevated (2.3-fold) compared with that after exposure to 5.6 mM glucose (Fig. 5A). In contrast, glucagon secretion at 1.1 mM glucose was reduced by 74.6% (*Hnf1a*^{+/+} 0.31 fmol h⁻¹ islet⁻¹, *Hnf1a*^{-/-} 0.078

fmol h⁻¹ islet⁻¹, p < 0.05) in *Hnf1a*^{-/-} islets compared with *Hnf1a*^{+/+} islets (Fig. 5A). The elevation of glucose concentration (5.6 mM and 11 mM) exerted no additional inhibitory effect on glucagon secretion in *Hnf1a*^{-/-} islets (Fig. 5A). Glucagon content was significantly increased in *Hnf1a*^{-/-} islets compared with *Hnf1a*^{+/+} islets (Fig. 5B), and stimulation with 20 mM KCl significantly increased glucagon secretion in *Hnf1a*^{-/-} islets compared with *Hnf1a*^{+/+} islets (Fig. 5C). Therefore, the reduction of glucagon secretion at 1.1 mM glucose is unlikely due to decreased glucagon content in α -cells. Consistent with the results from 4-week-old mice, glucagon secretion at 1.1 mM glucose was significantly decreased in *Hnf1a*^{-/-} islets compared with that in *Hnf1a*^{+/+} islets (Fig. 5D). Taken together, these results indicate that HNF1 α deficiency leads to dysregulated glucagon secretion in response to hypoglycemia.



3.5. HNF1 α regulates SGLT1 expression in pancreatic α -cells

SGLT1 is selectively expressed in small intestinal villus cells, renal tubule cells, heart, and pancreatic α -cells [11,28–30]. Suga et al. reported that SGLT1 inhibition significantly suppressed glucagon secretion from islets at 1 mM glucose [11]. There is a conserved HNF1

binding site in the promoter region of *Slc5a1* (encoding SGLT1) (Fig. 6A). HNF1 α binds to the promoter region and activates transcription of *Slc5a1* in intestinal cells [31]. Accordingly, we investigated whether HNF1 α controls glucagon secretion by regulating SGLT1 expression. First, we examined the recruitment of HNF1 α to the HNF1 binding site in the *Slc5a1* promoter region in α TC1-6 cells, a pancreatic

Fig. 6. SGLT1 is a direct target of HNF1 α in α -cells. (A) Multiple sequence alignment of mammalian *Slc5a1* promoters, depicting the high degree of conservation of the HNF1 binding motif. Alignments were generated by using CLUSTALW (<https://www.genome.jp/tools-bin/clustalw>). The arrow denotes the transcription start site. Highly conserved nucleotide sequences among species are indicated by an asterisk (*). (B) Binding of HNF1 α to the mouse *Slc5a1* gene promoter. ChIP-qPCR analysis was performed using 3 different primers: primer 1 (P1) targeted exon 3 of mouse *Tbp*, P2 targeted the mouse *Slc5a1* promoter without the HNF1 binding site, and P3 targeted the mouse *Slc5a1* promoter with the putative HNF1 binding site. Enrichment values at the indicated sites (P1–P3) were normalized to input DNA ($n = 5$). (C, D) qPCR and western blot analyses of SGLT expression in *Hnf1a* $^{+/+}$ and *Hnf1a* $^{-/-}$ mouse islets (C). qPCR and western blot analyses of SGLT expression in control shRNA and *Hnf1a* shRNA-overexpressing α TC1-6 cells (D). The relative expression levels of *Slc5a1* and *Slc5a2* were normalized to that of *Tbp* ($n = 3$). β -Actin was used as a loading control. (E) Dose-dependent effect of HNF1 α WT or HNF1 α dominant negative mutant P291fsinsC-*Hnf1a* on *Slc5a1* promoter activity. α TC1-6 cells were co-transfected with either 75 ng (square) or 150 ng (triangle) pcDNA3.1-HNF1 α WT or pcDNA3.1-P291fsinsC-*Hnf1a* expression vector, as well as 50 ng pGL4.10-*Slc5a1* promoter WT and 25 ng pRL-TK ($n = 4$). (F) Schematic diagram of a putative HNF1 binding site on the mouse *Slc5a1* promoter. The sequence of the binding mutant for HNF1 α is shown. α TC1-6 cells were co-transfected with 75 ng pcDNA3.1-*Hnf1a* WT, 50 ng pGL4.10 basic control or pGL4.10-*Slc5a1* promoter WT or pGL4.10-*Slc5a1* promoter mutant and 25 ng pRL-TK ($n = 4$). (G) *Slc5a1* promoter activity in control shRNA vs. *Hnf1a* KD α TC1-6 cells. The cells were co-transfected with 50 ng pGL4.10-*Slc5a1* promoter and 25 ng pRL-TK ($n = 4$). All data are presented as mean \pm S.E. (S.E.; error bars) * $p < 0.05$; ** $p < 0.01$; *** $p < 0.001$.

α -cell line, by a ChIP assay. Specific binding of HNF1 α to the promoter region of *Slc5a1* was identified in α TC1-6 cells (Fig. 6B). We then investigated whether *Slc5a1* transcription is dependent on HNF1 α in pancreatic α -cells. The expression of *Slc5a1* mRNA and SGLT1 protein was significantly decreased in the islets of *Hnf1a* $^{-/-}$ mice compared with those of *Hnf1a* $^{+/+}$ mice (Fig. 6C). It was reported that SGLT2 is expressed in pancreatic α -cells and controls glucagon secretion [29]. However, *Slc5a2* (encoding SGLT2) mRNA expression was not detected in islets (Fig. 6C) as reported in recent studies [11,32]. Knocking down *Hnf1a* expression led to the downregulation of SGLT1 expression in α TC1-6 cells without affecting *Slc5a2*, *Slc2a1* (encoding solute carrier family 2, member 1, GLUT1), and *Slc2a2* (encoding GLUT2) expression in α TC1-6 cells (Fig. 6D, Supplementary Fig. 3). The promoter region of the mouse *Slc5a1* gene was cloned into the pGL4-luciferase vector and co-transfected into α TC1-6 cells with WT-HNF1 α or P291fsinsC mutant-HNF1 α expression vectors. WT-HNF1 α activated the reporter gene, while P291fsinsC mutant-HNF1 α lacked transactivation activity (Fig. 6E). Mutation of the HNF1 α binding site in the reporter gene reduced (80.8% decrease, $p < 0.001$) the transactivation activity of HNF1 α (Fig. 6F). Furthermore, knocking down *Hnf1a* expression reduced reporter gene activity in α TC1-6 cells (Fig. 6G). These results indicate that HNF1 α regulates SGLT1 expression in pancreatic α -cells.

3.6. SGLT1 controls low glucose-stimulated glucagon secretion

We next investigated whether inhibition of SGLT1 affects glucagon secretion in α -cells. A fluorescent derivative of glucose, 2-NBDG, can be transported into living cells through SGLTs and GLUTs [33]. First, we examined 2-NBDG uptake in mouse islets at 1.1 mM glucose in the presence or absence of sotagliflozin, which is a non-selective SGLT inhibitor [34]. Pancreatic islets in mice are composed of an internal core of β -cells surrounded by a mantle of α -cells, which express GLUT1 and SGLT1 [11,35,36]. Fluorescence intensity was weak in the core of *Hnf1a* $^{+/+}$ islets, whereas strong intensity was detected in the periphery (rich in α -cells) (Fig. 7A). Interestingly, the fluorescence intensity in peripheral *Hnf1a* $^{+/+}$ cells was significantly reduced by 30.0% in the presence of sotagliflozin (Fig. 7A, B). In addition, peripheral fluorescence intensity was significantly decreased in *Hnf1a* $^{-/-}$ islets compared with that in *Hnf1a* $^{+/+}$ islets, and sotagliflozin treatment exerted no additional inhibitory effect (Fig. 7A, B). These results suggest that SGLT1 activates glucose uptake in α -cells under low glucose conditions. We then examined the effect of SGLT1 on glucagon secretion. Inhibition of SGLT1 in mouse islets by sotagliflozin and in α TC1-6 cells by siRNA significantly decreased glucagon secretion at 1.1 mM glucose (Fig. 7C–E). Glucagon secretion in the presence of low glucose was significantly reduced in *Hnf1a* $^{-/-}$ islets, coincident with decreased SGLT1 expression (Fig. 6C) compared with *Hnf1a* $^{+/+}$ islets (Fig. 7C). Notably, sotagliflozin did not exert an additional inhibitory effect in *Hnf1a* $^{-/-}$ islets (Fig. 7C). Similarly, *Hnf1a* knockdown in α TC1-6 cells led to a reduction of glucagon secretion at 1.1 mM glucose, and there was no additional decrease of glucagon secretion by

concomitant knockdown of *Slc5a1* (Fig. 7D, E). Collectively, these results indicate that SGLT1 inhibition suppresses glucagon secretion at low glucose conditions.

4. Discussion

Mutations in the gene encoding HNF1 α cause MODY3, which is associated with impaired insulin secretion. HNF1 α is expressed in pancreatic α -cells, but its role in these cells is unknown. In the present study, we revealed that the fasting glucagon levels of *Hnf1a* $^{-/-}$ mice were higher than those of control mice, and *Hnf1a* $^{-/-}$ mice exhibited inadequate suppression of glucagon after glucose load. Glucagon secretion is under paracrine control by insulin [8], and insulin secretion is severely impaired in *Hnf1a* $^{-/-}$ mice. The deficiency in insulin secretion in *Hnf1a* $^{-/-}$ β -cells might be responsible for the hypersecretion of glucagon observed in these mice. In agreement with these findings, a clinical study showed inappropriate glucagon suppression after glucose administration in patients with MODY3 [37]. The hypersecretion of glucagon might exacerbate postprandial hyperglycemia in *Hnf1a* $^{-/-}$ mice and in patients with MODY3.

Subjecting the mice to hyperinsulinemic hypoglycemia revealed that glucagon release was strikingly impaired in *Hnf1a* $^{-/-}$ mice compared with *Hnf1a* $^{+/+}$ mice. In addition, glucagon secretion at 1.1 mM glucose was also reduced in *Hnf1a* $^{-/-}$ islets. Consistent with our findings, Haliyur et al. reported that glucagon release after stimulation with low glucose and epinephrine was abrogated in the islets of a patient with MODY3 [10]. Further studies will be necessary, but these findings strongly suggest that HNF1 α deficiency causes impaired glucagon secretion as well as impaired insulin secretion. Patients with MODY3 often exhibit hypersensitivity to sulfonylureas compared with type 2 diabetic patients, and even low doses frequently result in hypoglycemia [38–40]. A dysfunction in glucagon secretion might exacerbate the risk of hypoglycemia in patients with MODY3. From a mechanistic point of view, we found that SGLT1 expression was decreased in *Hnf1a* $^{-/-}$ islets and in *Hnf1a* knockdown α TC1-6 cells. SGLT1 inhibition was reported to suppress glucagon release from isolated islets at 1 mM glucose [11]. Consistent with this report, we also found that 1.1 mM glucose-stimulated glucagon secretion was notably suppressed by SGLT1 inhibition. Low glucose activates voltage-dependent Na $^{+}$ channels and stimulates the amplitude of action potentials in pancreatic α -cells. This stimulates P/Q-type Ca $^{2+}$ -current activation and glucagon exocytosis [41,42]. At this point, we do not know the exact mechanism underlying the regulation of glucagon secretion by SGLT1, but the SGLT1 current carried by Na $^{+}$ co-transport is a depolarizing current. Inhibition of SGLT1 blocks the entry of positive Na $^{+}$ ions, and thus has a hyperpolarizing effect. Hyperpolarization could compromise glucagon secretion because the threshold for action potential generation will be not reached. In agreement with this idea, it was reported that the SGLT1 current is responsible for initiating electrical activity and glucagon-like peptide 1 secretion in intestinal L cells [43–45]. Meanwhile, ATP-sensitive potassium (K $_{ATP}$) channel activity

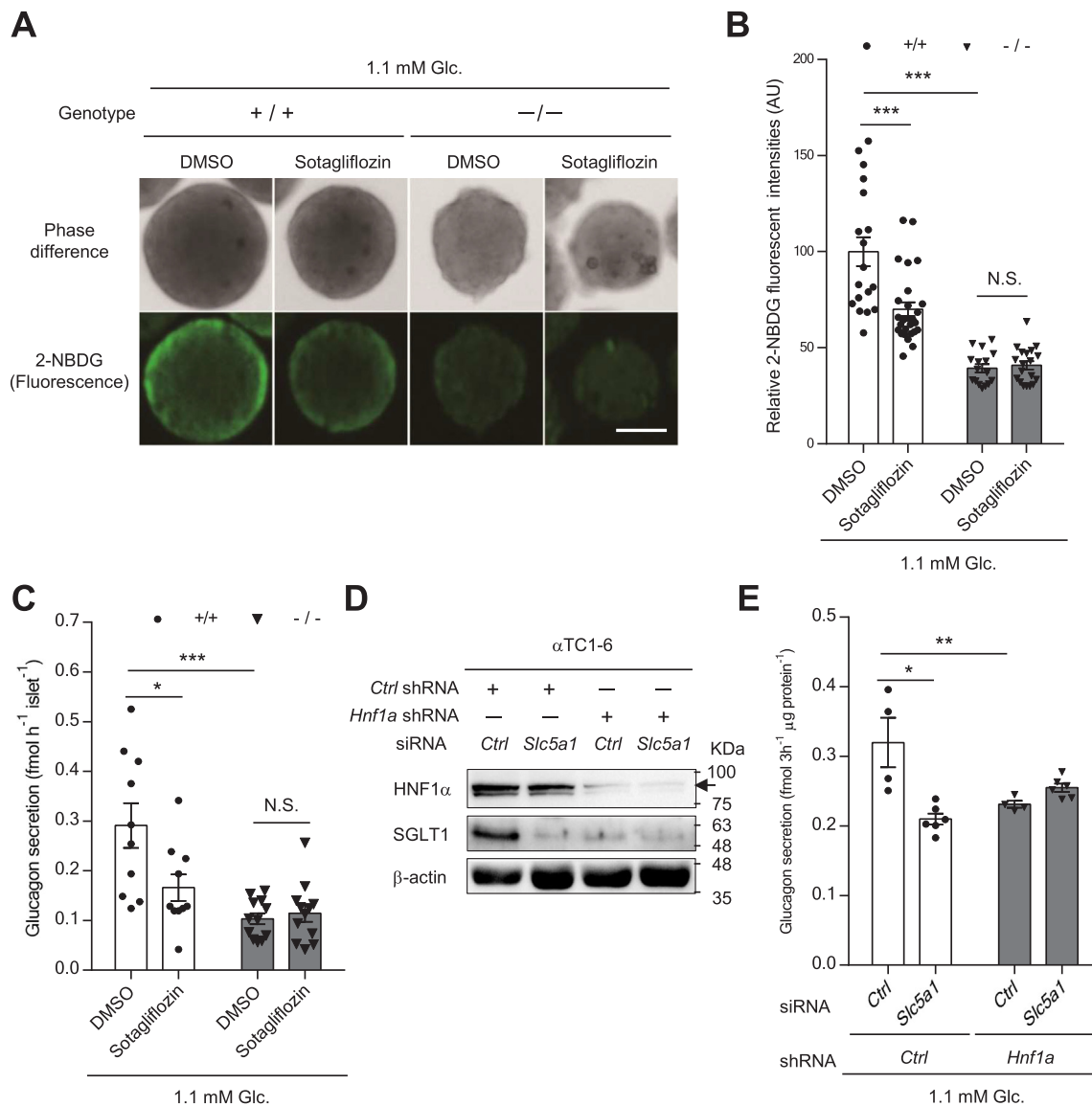


Fig. 7. Role of SGLT1 in the dysfunction of glucagon secretion in *Hnf1a*^{-/-} mouse islets and *Hnf1a* KD αTC1-6 cells. (A, B) Effect of sotagliflozin on 2-NBDG uptake in the islets of *Hnf1a*^{+/+} and *Hnf1a*^{-/-} mice at 1.1 mM glucose was evaluated. Representative light (top panel), and fluorescence (bottom panel) images of 2-NBDG-accumulated islets are presented (A), and quantification of relative 2-NBDG uptake at the periphery of the islets is shown (n = 16–18 islets from 2 to 3 mice per genotype). Scale bars, 50 μm (B). (C) Glucagon secretion at 1.1 mM glucose in isolated islets from *Hnf1a*^{+/+} and *Hnf1a*^{-/-} mice in the presence of DMSO or sotagliflozin was examined by ELISA (n = 10–12). (D) Western blot analyses of HNF1α and SGLT1 expression in control or *Hnf1a* KD αTC1-6 cells transfected with control siRNA or *Slc5a1* siRNA. β-Actin was used as a loading control. (E) The effect of *Slc5a1* knockdown on glucagon secretion at 1.1 mM glucose in control and *Hnf1a* KD αTC1-6 cells was examined (n = 4–6). Glucagon secretion for 3 h was normalized to total protein content. All data are presented as mean ± S.E. (S.E.; error bars) *p < 0.05; **p < 0.01; ***p < 0.001.

also plays an important role in glucagon secretion. Increased K_{ATP} channel activity as a result of metabolic disturbance (e.g., oligomycin treatment) leads to the loss of glucagon secretion at low glucose [41]. Indeed, K_{ATP} channel activity is increased in *Hnf1a*-deficient β-cells due to a defect in ATP production [46]. Thus, increased K_{ATP} channel activity might also be involved in the dysregulation of glucagon secretion in *Hnf1a*^{-/-} α-cells. Experiments with α-cell conditional *Hnf1a*^{-/-} mice and *Slc5a1*^{-/-} mice could provide additional useful information about the roles of HNF1α in α-cells.

Hnf1a^{-/-} mice exhibit a marked reduction of β-cell number with a reduced β-cell proliferation rate [5,6]. In contrast, we did not detect a significant decrease in α-cell area between *Hnf1a*^{+/+} and *Hnf1a*^{-/-} mice, suggesting that the contribution of HNF1α to cell growth is different between β- and α-cells. Furthermore, we found that ICCs, which consist exclusively of α-cells, were increased in the pancreas of

Hnf1a^{-/-} mice. It has been reported that hepatic glucagon signaling regulates α-cell proliferation [47,48]; however, the expression of *Gcgr* mRNA, which encodes the glucagon receptor, was unchanged in the liver of *Hnf1a*^{-/-} mice (data not shown). At present, the mechanism underlying this effect is unknown, but it might be worth noting that the ablation of HNF1α in human embryonic stem cells increases the development of α-cells *in vitro* [49].

In conclusion, we found that ICR *Hnf1a*^{-/-} mice are a novel model of human MODY3, and that HNF1α plays a critical role in proper glucagon secretion in mice. Further studies are necessary to determine whether the same abnormalities are characteristic of human MODY3. Detailed studies of ICR *Hnf1a*^{-/-} mice may lead to a better understanding of the molecular basis of glucagon secretion in patients with MODY3.

CRediT authorship contribution statement

Yoshifumi Sato: Conceptualization, Methodology, Writing - original draft, Investigation, Formal analysis. **Md Mostafizur Rahman:** Investigation, Formal analysis. **Masaki Haneda:** Investigation, Formal analysis. **Tomonori Tsuyama:** Investigation, Formal analysis. **Tomoya Mizumoto:** Investigation, Formal analysis. **Tatsuya Yoshizawa:** Investigation, Formal analysis. **Tadahiro Kitamura:** Writing - review & editing. **Frank J. Gonzalez:** Writing - review & editing. **Ken-ichi Yamamura:** Writing - review & editing. **Kazuya Yamagata:** Conceptualization, Methodology, Writing - original draft.

Declaration of competing interest

The authors declare that they have no known competing financial interest or personal relationships that could have appeared to influence the work reported in this paper.

Acknowledgements

The authors thank all the technical staff of laboratory for their assistance.

Funding

This study was supported by a Grant-in-Aid for Scientific Research (B) (19H03711), a grant from the Japan Agency for Medical Research and Development (JP19gm5010002), a grant from Japan Diabetes Foundation, and a grant from the Takeda Science Foundation.

Appendix A. Supplementary data

Supplementary data to this article can be found online at <https://doi.org/10.1016/j.bbadis.2020.165898>.

References

- [1] K. Yamagata, Roles of HNF1 α and HNF4 α in pancreatic β -cells: lessons from a monogenic form of diabetes (MODY), in: G. Litwack (Ed.), *Vitamins & Hormones*, vol. 95, Academic Press, Cambridge, USA, 2014, pp. 407–423.
- [2] K. Yamagata, N. Oda, P.J. Kaisaki, S. Menzel, F. Furuta, M. Vaxillaire, L. Southam, R.D. Cox, G.M. Lathrop, V.V. Boriraj, et al., Mutations in the hepatocyte nuclear factor-1 α gene in maturity-onset diabetes of the young (MODY3), *Nature* 384 (1996) 455–458.
- [3] M.M. Byrne, J. Sturis, S. Menzel, K. Yamagata, S.S. Fajans, M.J. Dronsfield, S.C. Bain, A.T. Hattersley, G. Velho, P. Froguel, et al., Altered insulin secretory responses to glucose in diabetic and nondiabetic subjects with mutations in the diabetes susceptibility gene MODY3 on chromosome 12, *Diabetes* 45 (11) (1996) 1503–1510.
- [4] M. Lehto, T. Tuomi, M. Mahtani, E. Widén, C. Forsblom, L. Sarelin, M. Gullström, B. Isomaa, M. Lehtovirta, A. Hykkö, et al., Characterization of the MODY3 phenotype. Early-onset diabetes caused by an insulin secretion defect, *J. Clin. Invest.* 99 (4) (1997) 582–591.
- [5] M. Pontoglio, S. Sreenan, M. Roe, W. Pugh, D. Ostrega, A. Doyen, A.J. Pick, A. Baldwin, G. Velho, P. Froguel, et al., Defective insulin secretion in hepatocyte nuclear factor-1 α -deficient mice, *J. Clin. Invest.* 101 (10) (1998) 2215–2222.
- [6] K. Yamagata, T. Nanno, M. Moriwaki, A. Ihara, K. Iizuka, Q. Yang, T. Satoh, M. Li, R. Uenaka, K. Okita, et al., Overexpression of dominant-negative mutant hepatocyte nuclear factor-1 α in pancreatic β -cells causes abnormal islet architecture with decreased expression of e-cadherin, reduced β -cell proliferation, and diabetes, *Diabetes* 51 (1) (2002) 114–123.
- [7] J.N. Walker, R. Ramrachea, Q. Zhang, P.R. Johnson, M. Braun, P. Rorsman, Regulation of glucagon secretion by glucose: paracrine, intrinsic or both? *Diabetes* 50 (1) (2001) 95–105.
- [8] D. Kawamori, A.J. Kurpad, J. Hu, C.W. Liew, J.L. Shih, E. Ford, P.L. Herrera, K.S. Polonsky, O.P. McGuinness, R. Kulkarni, et al., Insulin signaling in alpha cells modulates glucagon secretion in vivo, *Cell Metab.* 9 (4) (2009) 350–361.
- [9] T. Nanno, K. Yamagata, R. Hamaoka, Q. Zhu, T.E. Akiyama, F.J. Gonzalez, J. Miyagawa, Y. Matsuzawa, et al., Expression profile of MODY3/HNF-1 α protein in the developing mouse pancreas, *Diabetologia* 45 (2002) 1142–1153.
- [10] R. Haliyur, X. Tong, M. Sanyoura, S. Shrestha, J. Lindner, D.C. Saunders, R. Aramandla, G. Poffenberger, S.D. Redick, R. Bottino, et al., Human islets expressing HNF1A variant have defective β cell transcriptional regulatory networks, *J. Clin. Invest.* 129 (1) (2019) 246–251.
- [11] T. Suga, O. Kikuchi, M. Kobayashi, S. Matsui, H. Yokota-Hashimoto, E. Wada, D. Kohno, T. Sasaki, K. Takeuchi, S. Kakizaki, et al., SGLT1 in pancreatic α cells regulates glucagon secretion in mice, possibly explaining the distinct effects of SGLT2 inhibitors on plasma glucagon levels, *Mol. Metab.* 19 (2019) 1–12.
- [12] Y.H. Lee, B. Sauer, F.J. Gonzalez, Laron dwarfism and non-insulin dependent diabetes mellitus in the Hnf-1 α knockout mouse, *Mol. Cell. Biol.* 18 (5) (1998) 3059–3068.
- [13] T. Ohki, Y. Sato, T. Yoshizawa, K. Yamamura, K. Yamada, K. Yamagata, Identification of hepatocyte growth factor activator (Hgf) gene as a target of HNF1 α in mouse β -cells, *Biochem. Biophys. Res. Commun.* 425 (3) (2012) 619–624.
- [14] K. Araki, T. Imaizumi, T. Sekimoto, K. Yoshinobu, J. Yoshimuta, M. Akizuki, K. Miura, M. Araki, K. Yamamura, Exchangeable gene trap using the Cre/mutated lox system, *Cell. Mol. Biol.* 45 (1999) 737–750.
- [15] M. Mishina, K. Sakimura, Conditional gene targeting on the pure C57BL/6 genetic background, *Neurosci. Res.* 58 (2007) 105–112.
- [16] Y. Sato, T. Tsuyama, C. Sato, M.F. Karim, T. Yoshizawa, M. Inoue, K. Yamagata, Hypoxia reduces HNF4 α /MODY1 protein expression in pancreatic β -cells by activating AMP-activated protein kinase, *J. Biol. Chem.* 292 (21) (2017) 8716–8728.
- [17] Y. Sato, M. Inoue, T. Yoshizawa, K. Yamagata, Moderate hypoxia induces β -cell dysfunction with HIF-1-independent gene expression changes, *PLoS One* 9 (12) (2014) e114868.
- [18] T. Yoshizawa, M.F. Karim, Y. Sato, T. Senokuchi, K. Miyata, T. Fukuda, C. Go, M. Tasaki, K. Uchimura, T. Kadomatsu, et al., Sirt7 controls hepatic lipid metabolism by regulating the ubiquitin-proteasome pathway, *Cell Metab.* 19 (4) (2014) 712–721.
- [19] K. Yamagata, Q. Yang, K. Yamamoto, H. Iwahashi, J. Miyagawa, K. Okita, I. Yoshiuchi, J. Miyazaki, T. Noguchi, H. Nakajima, et al., Mutation P291fsinsC in the transcription factor hepatocyte nuclear factor-1 α is dominant negative, *Diabetes* 47 (8) (1998) 1231–1235.
- [20] M. Nishimoto, M. Katano, T. Yamagishi, T. Hishida, M. Kamon, A. Suzuki, M. Hirasaki, Y. Nabeshima, Y. Nabeshima, Y. Katsura, et al., In vivo function and evolution of the eutherian-specific pluripotency marker UTF1, *PLoS One* 8 (7) (2013) e68119.
- [21] M.F.W. Festing, Evidence should trump intuition by preferring inbred strains to outbred stocks in preclinical research, *ILAR J.* 55 (3) (2014) 399–404.
- [22] M. Pontoglio, Barra, M. Hadchouel, A. Doyen, C. Kress, J.P. Bach, C. Babinet, M. Yaniv, Hepatocyte nuclear factor 1 inactivation results in hepatic dysfunction, phenylketonuria, and renal fanconi syndrome, *Cell* 84 (4) (1996) 575–585.
- [23] T.E. Akiyama, J.M. Ward, F.J. Gonzalez, Regulation of the liver fatty acid-binding protein gene by hepatocyte nuclear factor 1 α (HNF1 α). Alterations in fatty acid homeostasis in HNF1 α -deficient mice, *J. Biol. Chem.* 275 (35) (2000) 27117–27122.
- [24] H. Hiraiwa, C.J. Pan, B. Lin, T.E. Akiyama, F.J. Gonzalez, J.Y. Chou, A molecular link between the common phenotypes of type 1 glycogen storage disease and HNF1 α -null mice, *J. Biol. Chem.* 276 (11) (2001) 7963–7967.
- [25] M.A. Garcia-Gonzalez, C. Carette, A. Bagattin, M. Chiral, M.P. Makinistoglu, S. Garbay, G. Prévost, C. Madaras, Y. Hérault, M. Leibovici, M. Pontoglio, A suppressor locus for MODY3-diabetes, *Sci. Rep.* 6 (2016) 33087.
- [26] K. Fukui, Q. Yang, Y. Cao, N. Takahashi, H. Hatakeyama, H. Wang, J. Wada, Y. Zhang, L. Marselli, T. Nanno, et al., The HNF-1 target collectrin controls insulin exocytosis by SNARE complex formation, *Cell Metab.* 2 (6) (2005) 373–384.
- [27] C. Watanabe, Y. Seino, H. Miyahira, M. Yamamoto, A. Fukami, N. Ozaki, Y. Takagishi, J. Sato, T. Fukuwatari, K. Shibata, et al., Remodeling of hepatic metabolism and hyperaminoacidemia in mice deficient in proglucagon-derived peptides, *Diabetes* 61 (1) (2012) 74–84.
- [28] V. Tsimihodimos, M. Elisaf, Effects of incretin-based therapies on renal function, *Eur. J. Pharmacol.* 818 (2018) 103–109.
- [29] C. Bonner, J. Kerr-Conte, V. Gmyr, G. Queniat, E. Moerman, J. Thévenet, C. Beauchamps, N. Delalleau, I. Popescu, W.J. Malaisse, et al., Inhibition of the glucose transporter SGLT2 with dapagliflozin in pancreatic alpha cells triggers glucagon secretion, *Nat. Med.* 21 (2015) 512–517.
- [30] L. Zhou, E.V. Cryan, M.R. D'Andrea, S. Belkowsky, B.R. Conway, K.T. Demarest, Human cardiomyocytes express high level of Na⁺/glucose cotransporter 1 (SGLT1), *J. Cell. Biochem.* 90 (2003) 339–346.
- [31] R. Kekuda, P. Saha, S. Sundaram, Role of Sp1 and HNF1 transcription factors in SGLT1 regulation during chronic intestinal inflammation, *Am. J. Physiol. Gastrointest. Liver Physiol.* 294 (6) (2008) G1354–G1361.
- [32] A. Solini, G. Sebastiani, L. Nigi, E. Santini, C. Rossi, F. Dotta, Dapagliflozin modulates glucagon secretion in an SGLT2-independent manner in murine alpha cells, *Diabetes Metab.* 43 (6) (2017) 512–520.
- [33] A.B. Blodgett, R.K. Kothinti, I. Kamyshko, D.H. Petering, S. Kumar, N.M. Tabatabai, A fluorescence method for measurement of glucose transport in kidney cells, *Diabetes Technol. Ther.* 13 (7) (2011) 743–751.
- [34] C.M.A. Cefalo, F. Cinti, S. Moffa, F. Impronta, G.P. Sorice, T. Mezza, A. Pontecorvi, A. Giaccari, Sotagliflozin, the first dual SGLT inhibitor: current outlook and perspectives, *Cardiovasc. Diabetol.* 18 (1) (2019) 20.
- [35] H. Heimberg, A. De Vos, D. Pipeleers, B. Thorens, F. Schuit, Differences in glucose transporter gene expression between rat pancreatic alpha- and beta-cells are correlated to differences in glucose transport but not in glucose utilization, *J. Biol. Chem.* 270 (15) (1995) 8971–8975.
- [36] R.E. Kuhre, S.M. Ghiasi, A.E. Adriaenssens, N.J. Wewer Albrechtsen, D.B. Andersen, A. Aivazidis, L. Chen, T. Mandrup-Poulsen, C. Ørskov, F.M. Gribble, F. Reimann, N. Wierup, B. Tyrberg, J.J. Holst, No direct effect of SGLT2 activity on glucagon secretion, *Diabetologia* 62 (6) (2019) 1011–1023.
- [37] S.H. Østoft, J.I. Bagger, T. Hansen, O. Pedersen, J.J. Holst, F.K. Knop, T. Vilsbøll,

- Incretin effect and glucagon responses to oral and intravenous glucose in patients with maturity-onset diabetes of the young-type 2 and type 3, *Diabetes*. 63 (8) (2014) 2838–2844.
- [38] T. Hansen, Eiberg, M. Rouard, M. Vaxillaire, A.M. Møller, S.K. Rasmussen, M. Fridberg, S.A. Urhammer, J.J. Holst, K. Almind, S.M. Echwald, L. Hansen, G.I. Bell, O. Pedersen, Novel MODY3 mutations in the hepatocyte nuclear factor-1alpha gene: evidence for a hyperexcitability of pancreatic beta-cells to intravenous secretagogues in a glucose-tolerant carrier of a P447L mutation, *Diabetes*. 46 (4) (1997) 726–730.
- [39] E.R. Pearson, B.J. Starkey, R.J. Powell, F.M. Gribble, P.M. Clark, A.T. Hattersley, Genetic cause of hyperglycaemia and response to treatment in diabetes, *Lancet*. 362 (9392) (2003) 1275–1281.
- [40] T. Tuomi, E.H. Honkanen, B. Isomaa, L. Sarelin, L.C. Groop, Improved prandial glucose control with lower risk of hypoglycemia with nateglinide than with glibenclamide in patients with maturity-onset diabetes of the young type 3, *Diabetes Care* 29 (2) (2006) 189–194.
- [41] Q. Zhang, R. Ramracheya, C. Lahmann, A. Tarasov, M. Bengtsson, O. Braha, M. Braun, M. Brereton, S. Collins, J. Galvanovskis, et al., Role of K-ATP channels in glucose-regulated glucagon secretion and impaired counterregulation in type 2 diabetes, *Cell Metab*. 18 (6) (2013) 871–882.
- [42] M.G. Pedersen, I. Ahlstedt, M.F.E.L. Hachmane, S.O. Göpel, Dapagliflozin stimulates glucagon secretion at high glucose: experiments and mathematical simulations of human A-cells, *Sci. Rep.* 6 (2016) 31214.
- [43] F.M. Gribble, L. Williams, A.K. Simpson, F. Reimann, A novel glucose-sensing mechanism contributing to glucagon-like peptide-1 secretion from the GLUTag cell line, *Diabetes*. 52 (5) (2003) 1147–1154.
- [44] H.E. Parker, A. Adriaenssens, G. Rogers, P. Richards, H. Koepsell, F. Reimann, F.M. Gribble, Predominant role of active versus facilitative glucose transport for glucagon-like peptide-1 secretion, *Diabetologia*. 55 (9) (2012) 2445–2455.
- [45] R.E. Kuhre, C.R. Frost, B. Svendsen, J.J. Holst, Molecular mechanisms of glucose-stimulated GLP-1 secretion from perfused rat small intestine, *Diabetes*. 64 (2) (2015) 370–382.
- [46] I.D. Dukes, S. Sreenan, M. Roe, M. Levisetti, Y.P. Zhou, D. Ostrega, G.I. Bell, M. Pontoglio, M. Yaniv, L. Philipson, K.S. Polonsky, Defective pancreatic beta-cell glycolytic signaling in hepatocyte nuclear factor-1alpha-deficient mice, *J. Biol. Chem.* 273 (38) (1998) 24457–24464.
- [47] R.W. Gelling, X.Q. Du, D.S. Dichmann, J. Romer, H. Huang, L. Cui, S. Obici, B. Tang, J.J. Holst, C. Fledelius, et al., Lower blood glucose, hyperglucagonemia, and pancreatic alpha cell hyperplasia in glucagon receptor knockout mice, *Proc. Natl. Acad. Sci. U. S. A.* 100 (3) (2003) 1438–1443.
- [48] C. Longuet, A.M. Robledo, E.D. Dean, C. Dai, S. Ali, I. McGuinness, V. de Chavez, P.M. Vuguin, M.J. Charron, A.C. Powers, D.J. Drucker, Liver-specific disruption of the murine glucagon receptor produces α -cell hyperplasia: evidence for a circulating α -cell growth factor, *Diabetes*. 62 (4) (2013) 1196–1205.
- [49] F.L. Cardenas-Diaz, C. Osorio-Quintero, M.A. Diaz-Mirand, S. Kishore, K. Leavens, C. Jobaliya, D. Stanescu, X. Ortiz-Gonzalez, C. Yoon, S. Chen, et al., Modeling monogenic diabetes using human ESCs reveals developmental and metabolic deficiencies caused by mutations in HNF1A, *Cell Stem Cell* 25 (2) (2019) 273–289.e5.